ENGINEERING RESEARCH INSTITUTE
UNIVERSITY OF MICHIGAN
ANN ARBOR

STUDY, DEVELOPMENT, AND PRODUCTION OF FERROSPINELS APPLICABLE TO TUNING OF SEARCH RECEIVERS

QUARTERLY PROGRESS REPORT NO. 4, TASK ORDER NO. EDG-6
Period Covering July 1, 1953 to September 30, 1953

Electronic Defense Group
Department of Electrical Engineering

By: D. M. Grimes
B. Hershenov
C. F. Jefferson
D. W. Martin
P. E. Nace
L. Thomassen

Approved by: H. W. Welch, Jr.
H. W. Welch, Jr.
Project Supervisor

Project 1970

CONTRACT NO. DA-36-039 sc-15358
SIGNAL CORPS, DEPARTMENT OF THE ARMY
DEPARTMENT OF ARMY PROJECT NO. 3-99-04-042
SIGNAL CORPS PROJECT 29-194B-0

October, 1953

TABLE OF CONTENTS

LIST OF ILLUSTRATIONS

TABLES I

TASK ORDER

Title: STUDY, DEVELOPMENT, AND PRODUCTION OF FERROSPINELS APPLICABLE TO TUNING OF SEARCH RECEIVERS

Purpose of Task:

To further the development of ferrospinels of different incremental permeabilities and low losses, with reference to specific applications of interest to the Signal Corps such as RF tuning units.

Procedure:

The approach to the general objective will include:

a. The preparation, under controlled conditions, of specimens of different compositions;

b. The measurement of parameters such as the incremental and initial permeabilities, the saturation inductance, the coercive force and the Q (figure of merit) at various frequencies;

c. The interpretation of these magnetic parameters in terms of the composition, reaction temperature, pressure and other conditions in the preparation of the samples;

d. The relationship of the solid state properties of the crystallite with the various measured magnetic parameters;

e. Theoretical explanations, where possible, for the relationships found in d. above.

Reports and Conferences:

a. Quarterly Task Order Reports shall be submitted reporting technical detail and progress under this Task Order;

b. Task Order Technical Reports of a final summary type are in general desirable and shall be prepared at the conclusion of investigations of each major phase. Such reports shall be prepared as decided in conference between the Electronic Defense Group and the Contracting Officer's Technical Representative in the Countermeasures Branch, Evans Signal Laboratory.

Personnel:

Electronic Defense Group:

Project Physicist: Mr. D. M. Grimes

Countermeasures Branch, Evans Signal Laboratory:

Project Engineer: Mr. Leon I. Mond

Components and Materials Branch, Squier Signal Laboratory

Project Scientist: Dr. E. Both

Comments:

The classification of this Task Order as Unclassified shall not preclude the classification of individual reports according to the information they contain, as determined in conference with the Contracting Officer's Technical Representative.

M. KEISER
Chief, Countermeasures Branch
Contracting Officer's Technical Representative

ABSTRACT

Theoretical work on an extension of the reversible magnetization to include the entire J-H loop is described. "Tuning Catastrophe" is described and predicted under certain conditions. Our technique for making ferrites is described, together with the results of permeability measurements on these cores at various frequencies.

STUDY, DEVELOPMENT, AND PRODUCTION OF FERROSPINELS APPLICABLE TO TUNING OF SEARCH RECEIVERS

QUARTERLY PROGRESS REPORT NO. 4, TASK ORDER NO. EDG-6
Period Covering July 1, 1953 to September 30, 1953

1. PURPOSE

The purpose of this report is to summarize the progress made by Task Group 6 of the Electronic Defense Group from July 1, 1953 to September 30, 1953 on the Signal Corps Contract No. DA-36-039 sc-15358.

The purpose of the task is to further the development of ferrospinels of different incremental permeabilities and low losses, with reference to specific applications of interest to the Signal Corps such as r-f tuning units.

The proposed program of Task Group EDG-6 was outlined in previous progress reports. Only those items will now be reported which have been worked on during the period.

2. PUBLICATIONS AND REPORTS

Mr. Paul Nace attended the National Electronics Conference in Chicago on September 28, 1953. No publications were issued during the quarter.

3. FACTUAL DATA

3.1 Theoretical J-H Loop (D. M. Grimes)

It has become necessary to alter the simple procedure of Sec. 4.1, QPR No. 3.

Our object now is to attempt to first of all describe the J-H loop, and then to obtain an expression for it. Once this is gotten it is hoped that χ_o will follow from it.

To obtain the J-H loop we first note, as is very well known, that for low fields magnetization occurs through wall movement, at high fields through rotation of the direction of magnetization inside a domain away from the easy directions. On the basis of Brown's work[1] (Eq. 12 of II) one is lead to an expression of the form:

$$\frac{J}{J_s} = \text{ctnh}\,\eta - \frac{1}{\eta}\;; \quad \eta = L_o H J_s \tag{1}$$

for the high field region. L_o is defined by $\chi = 1/3\ L_o J_s^2$. However Brown evaluates χ at H = J = 0, and thus obtains $\chi = \chi_o$. It would seem that the χ to be used here should be the χ which represents the susceptibility due to rotational processes rather than χ_o. However, χ_{rot} and χ_o are usually of the same order so the difference probably would not show up experimentally.

In the low field region the situation is complicated by "snagging" of the domain walls by internal potential energy minima. Without this snagging, the magnetization should be given by[1]: (Eq. 22 of II) - shown by the dashed curve of Fig. 1.

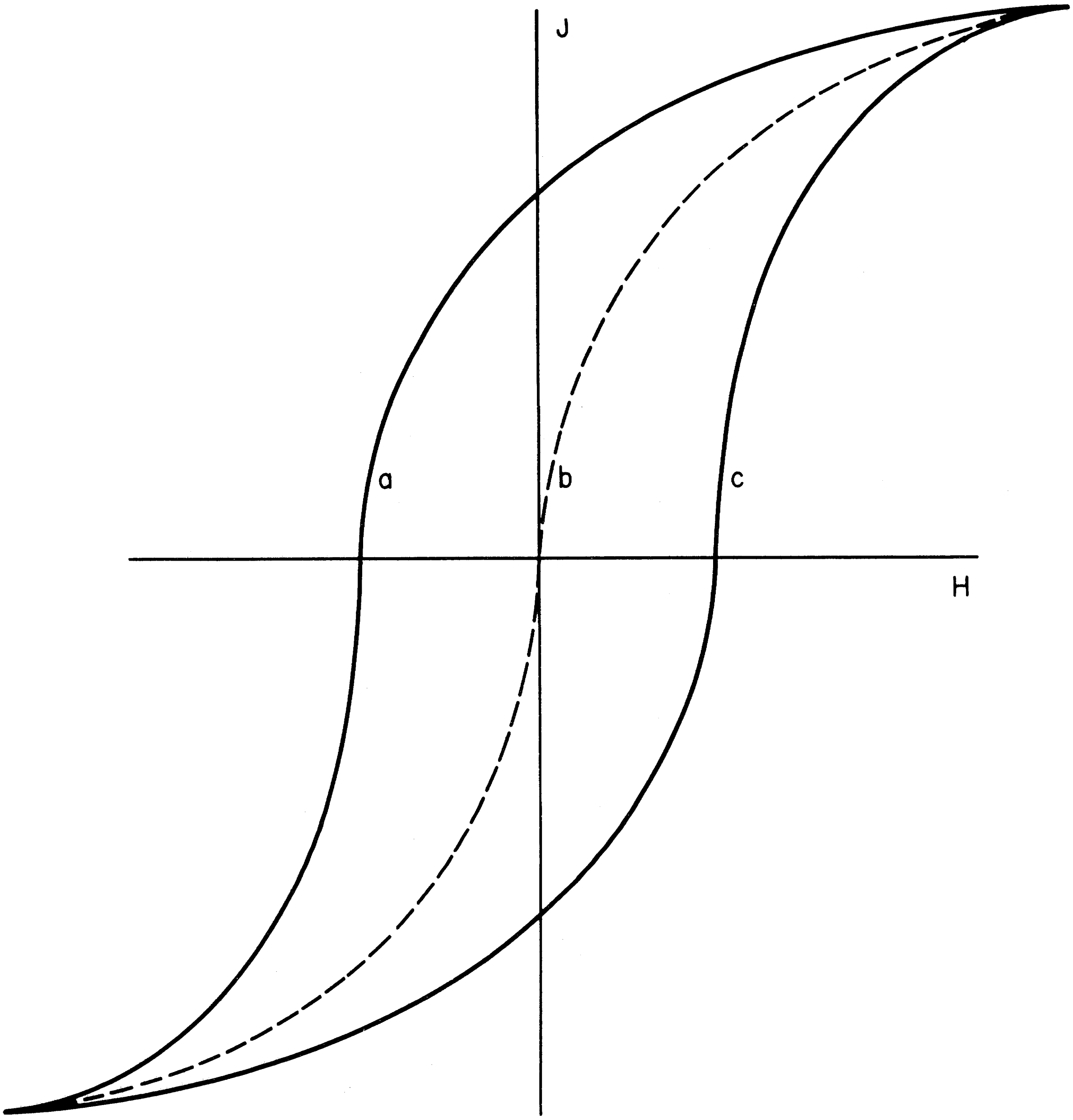

FIG 1

THE J-H LOOP

$$\frac{J}{J_s} = \frac{3}{\eta^2} \int_0^{\eta} \mu \tanh \mu \, d\mu$$

(2)

$$L = \frac{3\sqrt{3}\,\chi}{H J_s} \qquad \eta = \frac{L J_s H}{\sqrt{3}}$$

We now consider the question, what value of χ should be substituted into the value for L here. When going from H = $+\infty$ to $-\infty$, the value of J is always greater than it would be were there no "snagging". When wall movements start the walls are restricted by snags from moving freely. Thus curve "a" is traced out. The dashed curve, for H > 0 is a monotonic increasing function of H with a monotonic decreasing derivative. From simple arguments one can show that the maximum slope of the dashed curve must be very nearly equal to the maximum slope of line "a". The maximum slope of the dashed curve occurs at J = 0. Therefore in Eq. (2),

$$\eta = \frac{L J_s H}{\sqrt{3}} \quad \text{and} \quad L = \frac{3\sqrt{3}\,\chi_{max}}{J_s^2} \tag{2'}$$

where χ_{max} is the maximum slope of the J-H curve.

These expressions, Eq. (1) and Eq. (2), were derived by Brown for the case made reversible by considering only minute changes in H. In effect we are now assuming they apply equally well to a system made reversible by hypothesizing the non-existence of snags. This, however changes the boundary conditions so that χ_{max} appears in Eq. (2').

We note the "snagging" will in effect change the value of H in the argument of Eq. (2). The value of the displacement, i.e. if one assumes $\eta = \frac{LJ_s}{3}(H-H_o)$, the value of H_o, will depend upon the volume of material through which a wall would have passed but is restrained from doing so by the internal snags. This can be represented by a distribution function representing the number of "potential" holes with a depth within a given region.

The results of this model are currently being considered in some detail.

3.2 Tuning Catastrophe (D. M. Grimes; P. E. Nace)

Several mechanisms affect the frequency dependence of the permeability of ferrite material. These arise from the effective mass of the domain wall, from precession of the direction of orientation of the domains and from dimensional resonances. These result in a given μ - ω curve for a given specimen with a given geometry.

When one designs a tuning unit it is necessary to consider the above relationship between μ and ω in addition to the change in permeability of the material as a result of a change in its internal magnetization. It is intuitively obvious that, if μ decreases with ω, when J is increased in the core of a tuning unit causing μ to decrease and thus ω to increase, the frequency change is augmented by the original μ-ω relation. The result is a larger frequency range for the unit. We will now consider this quantitatively.

Consider μ as a function of ϕ and ω. ϕ can represent either magnetic biasing field or the internal magnetization. Thus:

$$\mu = \mu(\phi, \omega)$$

$$d\mu = \left(\frac{\partial \mu}{\partial \phi}\right)_\omega d\phi + \left(\frac{\partial \mu}{\partial \omega}\right)_\phi d\omega \qquad (1)$$

It should be emphasized that Eq. (1) is a property of the particular ferrite core.

If the permeability is measured by means of a parallel resonant circuit we have an additional relationship

$$\omega = \frac{1}{\sqrt{\mu L_o C}}$$

Define (2)

$$\omega_o = \frac{1}{\sqrt{L_o C}}$$

so

$$\mu = \frac{\omega_o^2}{\omega^2}$$

This gives:

$$d\mu = -\frac{2\mu}{\omega} d\omega \qquad (3)$$

Equations (2) and (3) are properties of the circuit into which the core is placed. Upon substituting (3) into (1), we obtain

$$\frac{d\ln\omega}{d\ln\phi} = -\frac{1}{2}\,\frac{\left(\partial\ln\mu/\partial\ln\phi\right)_\omega}{1 + \frac{1}{2}\left(\frac{\partial\ln\mu}{\partial\ln\omega}\right)_\phi} \qquad (4)$$

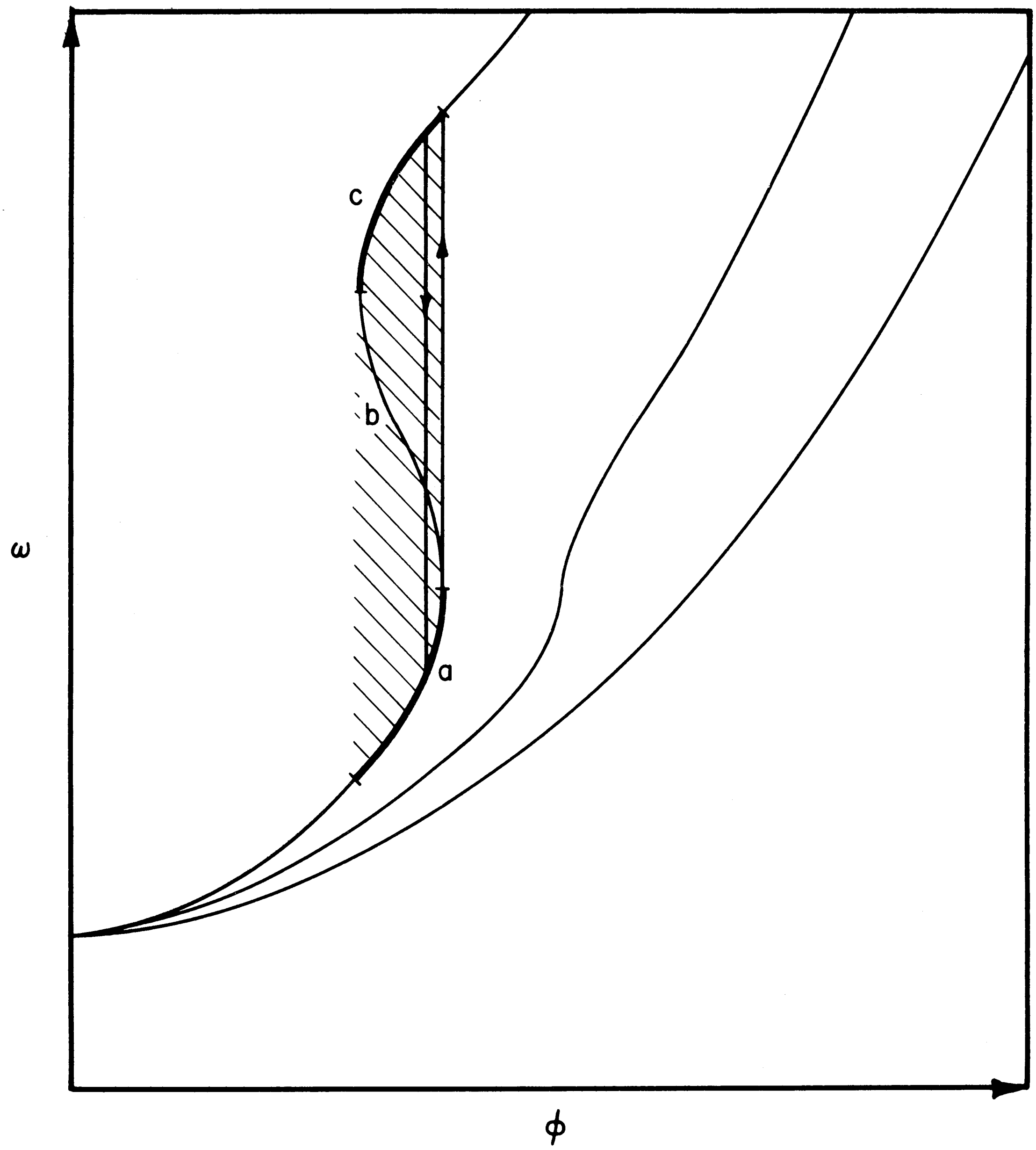

FIG 2

TUNING CURVES FOR DIFFERENT μ-ω SPECTRA

Note that if $\frac{1}{2} \left(\frac{\partial \ln\mu}{\partial \ln\omega}\right)_\phi < -1$, the slope of the ω-ϕ curve becomes infinite.

A family of curves (ω-ϕ) is plotted in Fig. 2 for different μ-ω spectra. Curve "b" in the shaded area represents a decreasing frequency for a decreasing magnetization. It can have no physical significance. If the oscillations are not large enough for the oscillations on line "a" to alter line "c" both frequencies may be present at the same time. In this case the frequency which suffers the largest loss, usually the higher frequency, will soon be damped out. Thus the path to be expected is that shown by the arrows.

This effect could lead to holes in the frequency spectrum the receiver is being swept over.

We will call the above discontinuity the tuning catastrophe.

There is nothing in the above equations to limit them to ferrites. They would be equally applicable to ferromagnetic material. Also μ could be replaced by ϵ and the equations would be valid for the ferroelectrics.

3.3 Transverse Permeability and Saturation Magnetization
(D. W. Martin; D. M. Grimes)

A considerable difficulty encountered in magnetic measurements is the "demagnetizing field" induced in a specimen by free poles appearing at its surface when it is magnetized. This field is roughly proportional to the magnetization, where the proportionality constant N is dependent upon the shape of the specimen. N can range from zero, for special geometries, up to the value 4π for the limiting case of an infinitely short cylinder magnetized along its axis. In this instance, the demagnetizing field entirely cancels any applied field within the cylinder, and there can be no magnetization at all.

Transversally, a toroidal core is essentially a disk, or very short cylinder. It is estimated that its "demagnetizing factor" $\frac{N}{4\pi}$ is about 0.8, although it is not precisely known, and is really not even a constant. To see how this will effect measurements, let the true field H be given by:

$$H = H_o - NJ$$

where H_o is the applied field, and J the magnetization. Then

$$\begin{aligned} 4\pi J &= (B - H) \\ &= (B - H_o)/\left(1- \frac{N}{4\pi}\right) \end{aligned} \tag{1}$$

so the true J would be 5 times as great as the apparent magnetization, $J_a = (B - H_o)/4\pi$ for $\frac{N}{4\pi} = 0.8$. Even more drastic is the effect on the applied field necessary for a given degree of magnetization. For:

$$\begin{aligned} H_o &= H + NJ \\ &= \left[1 + \frac{N}{4\pi}(\mu - 1)\right] H \end{aligned}$$

If μ is large and $\frac{N}{4\pi}$ is not almost zero,

$$H_o \cong \frac{N}{4\pi} \mu H \tag{2}$$

which may be larger than H by whole orders of magnitude.

If the pole faces of the external magnet make perfect magnetic contact with the specimen surface, and the yoke provides a zero-reluctance path outside the sample for the flux, then ideally the effective demagnetizing factor will be reduced to zero. The new magnet mentioned in QPR No. 3, and now in service, was designed for this purpose. It has accurately parallel plane pole faces, of diameter over 40% greater than the core diameter, and the gap is continuously variable from zero to about 1 cm. To check its effectiveness, an old core has been fitted with a groove to hold the leads from the inside girdle winding, so that the latter do not project above the surface. Thus measurements could be made with both pole faces in firm contact with the core surfaces. The apparent J_s of the core was then measured by the method of QPR No. 3, Sec. 4.2 with this geometry, as well as with several different gaps between core and pole face. In fig. 3, the apparent J_s (in arbitrary units) is plotted against the height of this gap. It is seen that the curve rises sharply near the nominal zero, so that true J_s (for perfect contact) is rather indeterminate. Further steps such as careful polishing of core surfaces, or filling the space between surfaces with a ferromagnetic dust, must be attempted in order to pin down a reproducible zero gap.

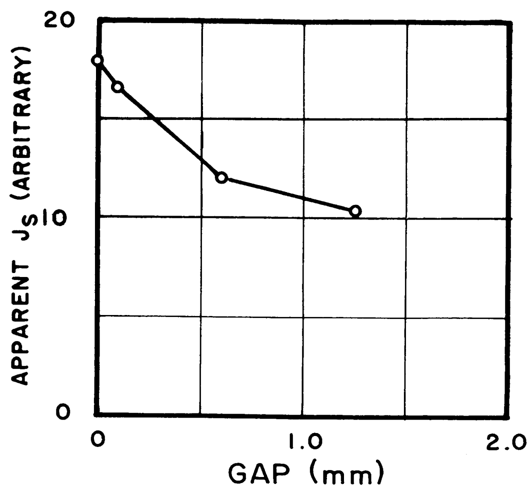

FIG 3

APPARENT J_S VS MAGNET GAP

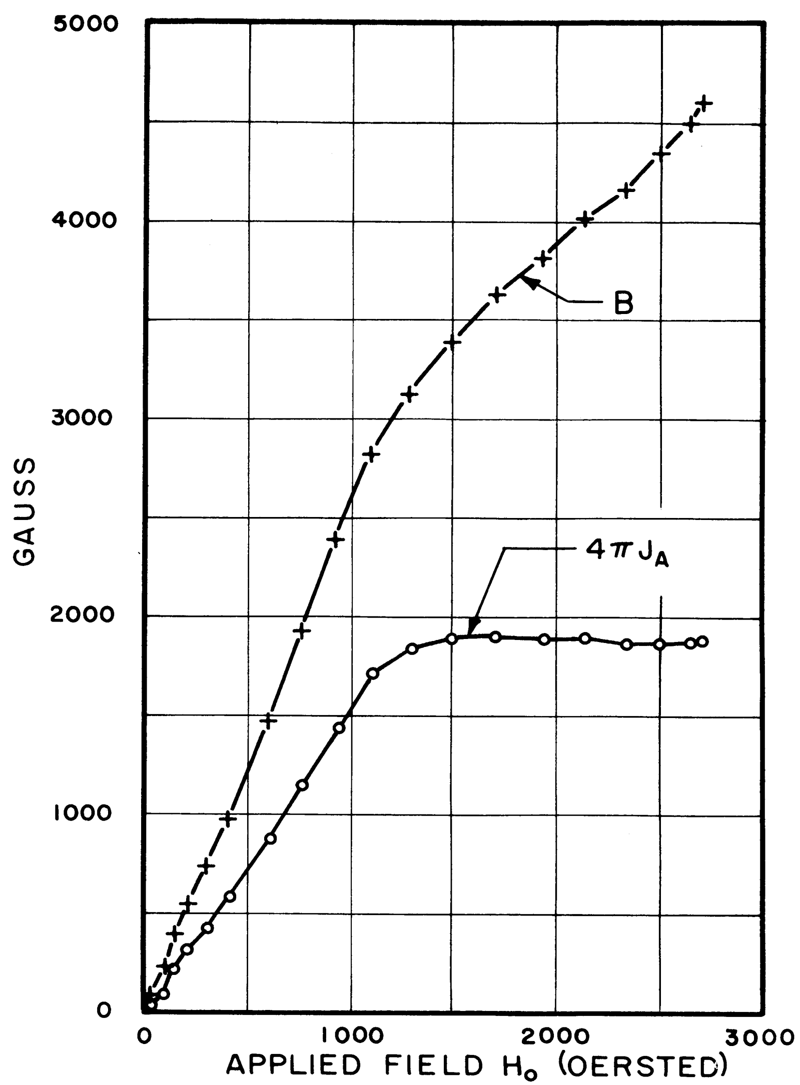

FIG 4

B AND APPARENT J VS APPLIED FIELD

Although the windings are of No. 34 wire, the total area embraced by the B winding is several percent greater than the core area. Since the applied field is large, of the same order as B (eq. 2), the flux through this additional area constitutes an appreciable correction to B.

Fig. 4 shows part of the B and $\{4\pi J_a = (B - H_o)\}$ vs. H_o curve of core GC-G5 for a geometry in which there are equal gaps on each side of the core, each of about 1/2 the sample thickness. Note that, with the above correction, the J_a curve levels off nicely beyond saturation. The saturation value of 1890 for $4\pi J_a$ would be consistent with the parallel field value of 3400 if we take for the effective demagnetizing factor

$$\frac{N}{4\pi} = 1 - \frac{1890}{3400} = 0.44$$

It should be emphasized that the abscissa of Fig. 4 is the applied field H_o. The true field H given by

$$H = H_o - NJ$$

$$= \frac{H_o}{1 - \frac{N}{4\pi}} - \frac{B}{\frac{4\pi}{N} - 1}$$

is essentially unknown, since it is a small difference of two large terms. It is zero within experimental error up to the base of the curve, beyond which it increases rapidly up to about 1500 oersted.

The apparent J_s of this core has been found for several geometries, and each can be made to agree with the parallel data by a reasonable and consistent value of $\frac{N}{4\pi}$. One preliminary recheck of the transverse incremental permeability has been done so far, by the method of QPR No. 2, using the new magnet. In this method, it is assumed that $4\pi J_s$ is essentially equal to the measured B at which μ_Δ reaches its minimum, since H should be much smaller. In QPR No. 3 it is stated that this gives J_s values some 50% larger than do the parallel measurements. The present readings give a value still somewhat large, but much less so. It would appear that the improved homogeneity of the field is probably responsible. So it appears at present that the difference in J_s for the two directions is not real. Further study is in order to refine the methods and the corrections to settle the question fully.

The present fluxmeter is found to be too sensitive. It must be shunted to stay on scale, and presents annoying drift problems. A less sensitive instrument has been ordered, which will help reduce experimental uncertainties. We believe that this and other refinements of technique will soon permit definite answers to some of the questions. Issuance of the Technical Report on the Theory of Reversible Susceptibility must await these developments.

3.4 Manufacture of the Ferrites (C. F. Jefferson; L. Thomassen)

3.4.1 Equipment. The Harper Electric furnace, Model HL-6 arrived early in the quarter. The oven has a maximum temperature variation of 10° C at 1200° C when it is set on thermostatic control. The rate of heating and cooling is controlled by manually regulating a multiple tap transformer. The General Electric Reactrol system is being investigated as a means of automatically regulating the power input.

A 10 ton hydraulic laboratory press was obtained to use in pressing the cores. A heavier press is available for higher pressures.

It was found that there was a considerable amount of magnetic material in the nickel oxide. A magnetic separator was constructed in the laboratory for removing it.

The die used for pressing the cores has been modified to facilitate removal of the core from the die. Fig. 5 shows the die now in use.

3.4.2 Manufacture. The search for a better method of mixing the oxides is being continued. A high-speed mixer was tried, but since it was found that the mixer did not crush the lumps in the oxides the possibility of using an ultrasonic vibrator as a means of mixing the oxides is being investigated. Until a more satisfactory method is found the oxides will be mixed in the ball mill.

Most of the cores made prior to this quarter were made without the use of a binder. This was done in order to reduce the number of variables in the preparation of the cores. Now that a greater number of cores are being made it has been found necessary to use a binder to lubricate the die and facilitate removal of the cores from the die. Several binders were tried, such as aerosol, carbowax and ammonium oleate. Ammonium oleate has proven to be the most satisfactory binder tried to date. This

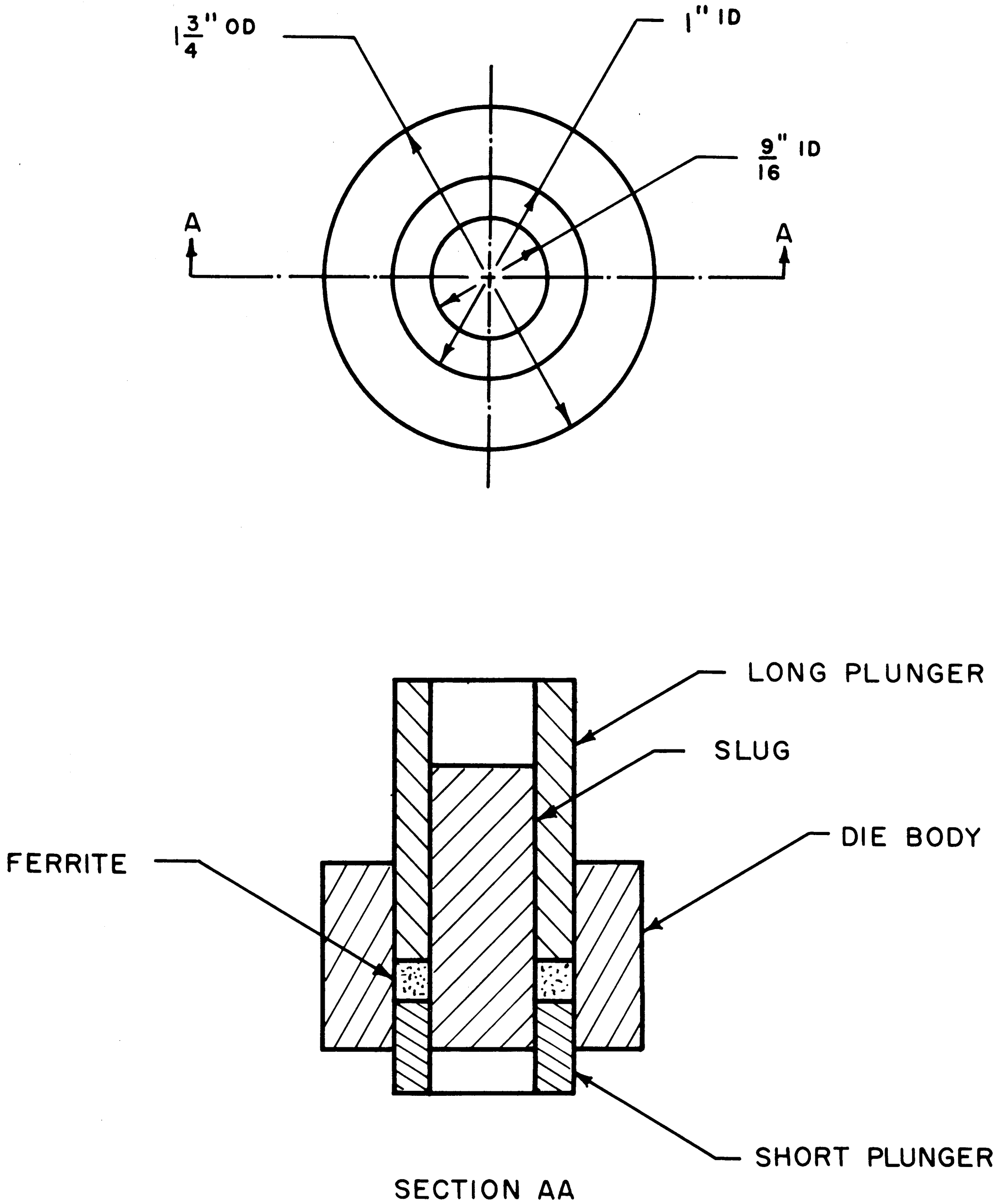

FIG 5

FERRITE DIE

binder works remarkably well under high pressing pressure. Pressing pressures as high as 40 tons/ sq. inch have been used on specimens 2.2 mm thick without laminations. No higher pressures have been tried. No attempt has been made to evaluate the effect of the various binders on the fired core. All binders were evaluated only insofar as they effected the pressing operation.

Cores have been made using pressing pressures of from 2 to 40 tons/ sq. inch. The density of the cores were calculated from the volume and weight of the cores. There does not appear to be any increase in density as the pressure is increased. There is, however, a considerable change in the percentage of linear shrinkage as the pressure changes:

PRESSURE (tons/sq.inch)	% LINEAR SHRINKAGE	DENSITY
2	20.5	4.75
16	13.4	4.75
20	12.2	4.80
30	11.2	4.75
40	10.5	4.80

Micrographs of cores pressed at 2, 10 and 20 tons/ sq. inch were made. No distinction could be made between the cores as far as the voids were concerned.

The oven is so arranged that the cores can be fired in an atmosphere of oxygen. The oxygen flow is regulated with a gas flow meter. The oxygen is introduced into the oven through a vycor tube placed in the chamber.

3.4.3 Metalographic Polishing. The ferrite material is difficult to etch. It has been found that the grain boundries can be brought out, however, by etching for 1 minute in a boiling solution of .05 N $SnCl_2$ in concentrated hydrochloric acid.

3.5 Chemical Analysis (C. F. Jefferson)

An analysis of a ferrite material for nickel and iron was obtained from the National Spectrographic Laboratories. From the values obtained, the per cent of O_2 was determined by difference. This calculation indicated that the material was deficient in oxygen. This would indicate that some of the cations were present in a reduced state. For this reason it was desired to determine the amount of ferrous iron present in the material directly.

The most direct method would be to dissolve the ferrite in HCl under a CO_2 atmosphere and titrate the ferrous iron with potassium dichromate. It was found, however that none of the common solvents would dissolve the ferrite. The ferrite was even insoluble in HF. The only convenient method found to dissolve the material was to use $SnCl_2$ in HCl. For this reason the following method was used:

The material was dissolved in a standardized solution of $SnCl_2$ in HCl under a CO_2 atmosphere. After the material was dissolved, the amount of ferric iron was determined by titration with the same standard solution of $SnCl_2$. The total iron was then determined in the same sample using the potassium dichromate method. The amount of ferrous iron was then calculated as the difference between the total iron and the ferric iron.

An analysis of ferrous iron by the above procedure on the same sample submitted to the National Spectrographic Co. showed no ferrous iron present.

In order to check the above procedure, a laboratory now running routine ferrous analysis has agreed to make a determination on several samples for us.

3.6 Low and Mid-Frequency Permeability Spectrum (B. Hershenov)

3.6.1 Permeameter Measurements. The primary core for the 4-9 mc/s range in the r.f. permeameter arrived this quarter. The core shipped previously was returned because the capacitance in the primary windings was too large. At 7 mc/s with this core, the permeameter yielded capacitive readings with the secondary opened. The cores that have been manufactured here have all been measured in the frequency range spanned by the permeameter cores. Table I indicates the results of four of the recent cores all manufactured under different conditions, as compared with the results of specimen A-5-2 reported in the last progress report and two cores, 305 and 306, General Ceramics G bodies furnished by the Mr. G. Dewitz of the C.G.S. Laboratories. 305 was listed as satisfactory and 306 as having a low Q. Within any one group of cores, such as A-16, all the cores yielded about the same values for μ_1 and μ_2. The notable exceptions to this were the specimens in groups A-21 and A-22. At the lower frequencies μ_1 varied as much as 200, while

TABLE I

SPECIMEN	$f=1.2x10^6$cps		$f=4x10^6$		$f=7x10^6$cps	
	μ_1	μ_2	μ_1	μ_2	μ_1	μ_2
A-5-2	334	66	324	250	262	227
A-16-1	184	12	212	50	201	81
A-17-4	400	36	475	238	367	237
A-21-1	681	98	774	638	637	718
A-22-2	680	74	763	540	633	525
305	345	9	430	129	428	272
306	357	30	431	141	380	208

COMPLEX PERMEABILITY FOR SEVERAL SPECIMENS at the higher frequency μ_2 varied by as much as 200. The specimens in this group were pressed at a load of one ton (approximately 2 tons/in^2) as opposed to the other cores which were pressed at loads ranging from 8 to 20 tons. At the lower frequencies μ_1 is relatively high and remains high at the upper frequencies, but μ_2 increases rapidly with frequency.

3.6.2 Extension of Permeameter Range. A recent communication from P.H.Haas of Magnetic Measurements and Standards Section, National Bureau of Standards, indicates that coils are now available for the r.f. permeameter which will extend its upper limit to 20 mc/s. These coils can be used without correction for capacitance in the primary windings. The National Electronics Labs. has informed us that cores will soon be available which will extend the lower limit of the permeameter to 100 kc. Orders have been placed for both type cores with delivery in about six weeks.

3.7 VHF Permeability Spectrum (P. E. Nace)

3.7.1 Analysis of data obtained. Measurements of the permeability and Q in the frequency range from 30 to 500 mc/sec. have been made in the past quarter on a selected number of our ferrite cores. These cores exhibited almost identical vhf permeability curves although they were subjected to different manufacturing processes. All the cores were 20-30 nickel-zinc cores with some containing 0.75 mole per cent V_2O_5. Of all the manufacturing parameters involved only one had an appreciable effect on the vhf permeability. Those cores which were prefired had lower permeability, lower losses, but higher Q. These prefired cores are quantitatively and qualitatively in agreement with Fig. 5 of QPR No. 3. Those cores which were not prefired showed higher permeability and losses, but lower Q. Fig. 6 shows the range of μ_1 and μ_2 observed for eleven of our cores. These cores were subjected to different manufacturing processes, but none were prefired; all were 20-30 Ni-Zn cores, and all contained either zero or 0.75 mole per cent of V_2O_5. Also falling in this range were two types of General Ceramic G-body cores obtained from Mr. G. Dewitz of the C.G.S. Laboratories. One of the two was deemed satisfactory; the other was considered by Mr. Dewitz to have too low a Q at 1 mc/s to be satisfactory. Fig. 6 indicates that the manufacturing parameters other than prefiring have little effect on the vhf permeability. All these data were obtained with the coaxial inductor described in QPR No. 3.

3.7.2 The Coaxial Line. A coaxial line for measuring permeability, magnetic losses, dielectric constant, and conductivity of toroidal specimens has been constructed. Fig. 7 is an assembly drawing of the coaxial line. Flexible inner and outer conductors will allow a small range of toroidal core sizes to be measured. The inner conductor is compressed by the core. The outer conductor is compressed by a hose clamp. Thereby a given core is mounted with the inner and outer conductors fitting tightly on the inner and outer radii of the core. The characteristic impedance of the line is not altered if the ratio of the

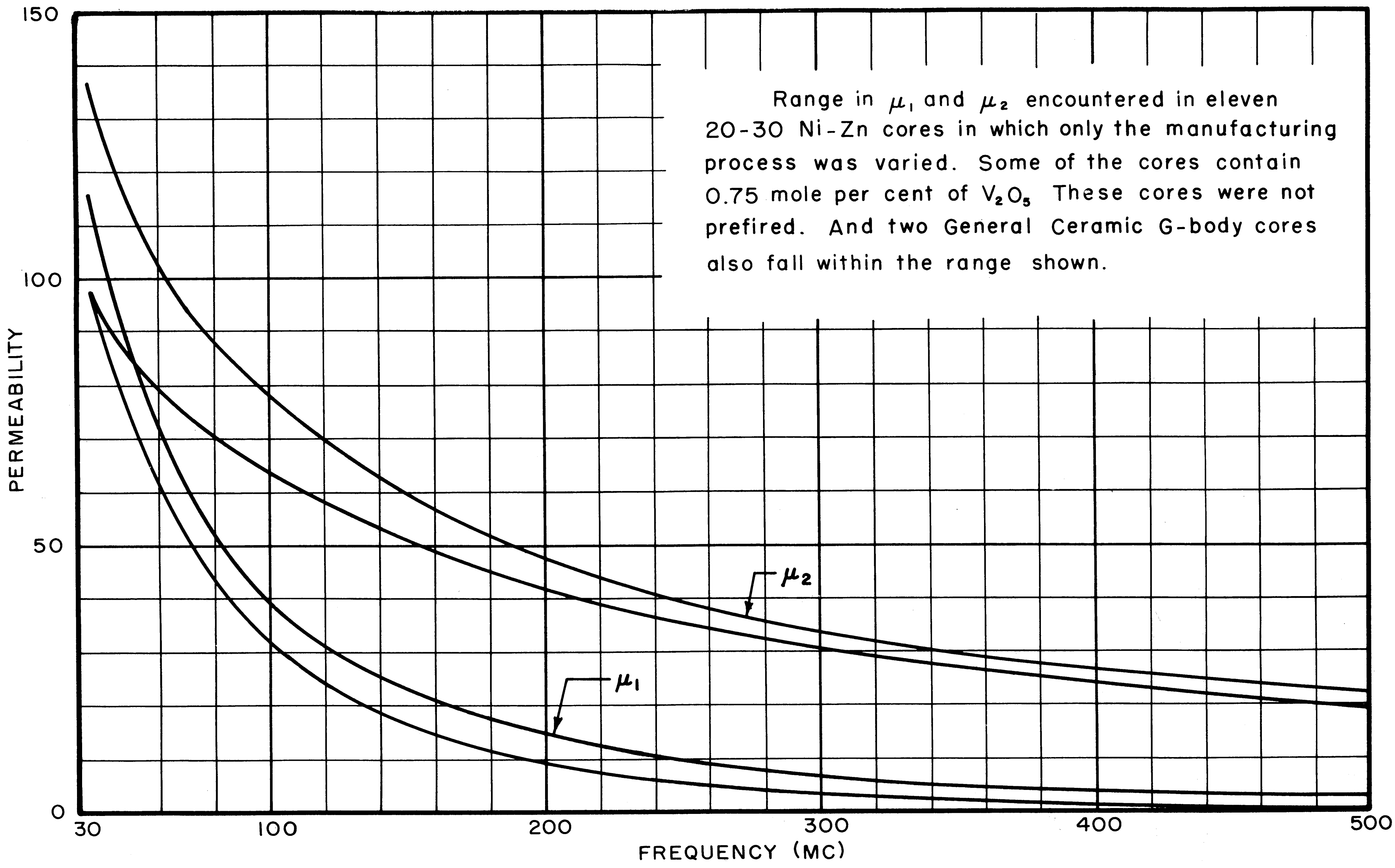

FIG 6

VHF PERMEABILITY SPECTRUM

M-970 A-G6-39 RFR 26OCT 53

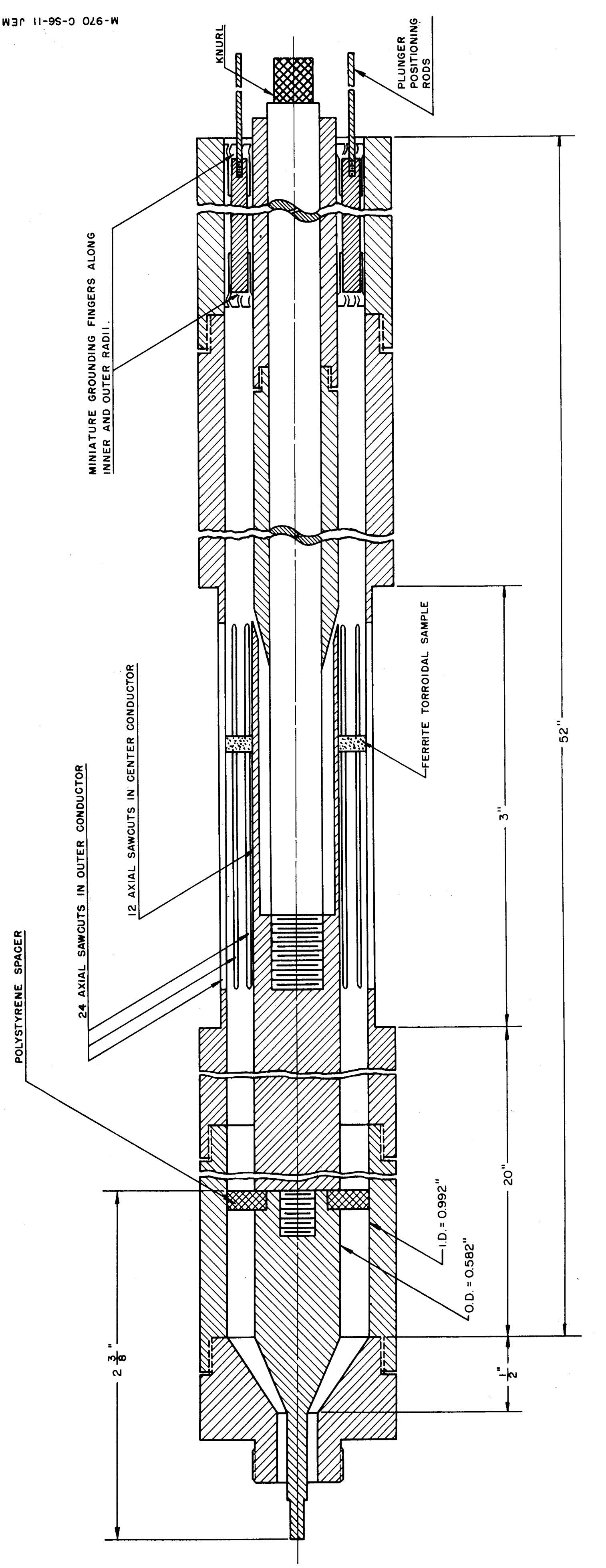

FIG. 7

COAXIAL LINE ASSEMBLY.

inner and outer radii is maintained. This ratio is essentially constant for our cores, and the line was designed with the same ratio for the inner and outer conductor radii.

$$Z_o = 60 \ln \frac{r_o}{r_i} = 60 \ln \frac{.992''}{.582''} = 32 \text{ ohms}$$

For an ideal coaxial line the procedure of measurement would be as follows:

(1) Position the shorting plunger adjacent to the ferrite ring and measure the impedance and phase angle by means of the Hewlett-Packard vhf bridge.

(2) Correct the observed reading by means of the Z-ϕ chart because of a short length (about 8 cm) of 50 ohm coax joining the coaxial line to the bridge. This gives the impedance at the input end of the coaxial line.

(3) Use the Z-ϕ chart to transfer the latter impedance into the impedance in the coaxial line at the bridge face of the ferrite toroid. This impedance[2] $Z_{f1}e^{j\phi f1} = Z_{of} \tanh \gamma_f t_f$ where Z_{of} (1) is the characteristic impedance of a coaxial line with a ferrite dielectric and γ_f is the propagation constant in the ferrite. t_f is the thickness of the ferrite sample.

(4) Reposition the shorting plunger 1/4 wavelength from the ferrite sample. Measure the impedance and repeat steps 2 and 3, thereby[2] determining $Z_{f2}e^{j\phi f2}$

$$Z_{f2}e^{j\phi 2} = Z_{of} \coth \gamma_f t_f \qquad (2)$$

(5) From equations (1) and (2), Z_{of} and γ_f can be determined:

$$Z_{of} = (Z_{f_1} Z_{f_2})^{\frac{1}{2}} e^{(\phi_{f_1} + \phi_{f_2})/2} \tag{3}$$

$$\gamma_f = \frac{1}{t_f} \tanh^{-1} \left(\frac{Z_{f_1}}{Z_{f_2}}\right)^{\frac{1}{2}} e^{\frac{j}{2}(\phi_{f_1} - \phi_{f_2})} \tag{4}$$

(6) For a coaxial line[3]: $\gamma_f = j\omega \sqrt{\mu_f \epsilon_f}$ (5)

$$Z_{of} = \frac{1}{2\pi} \sqrt{\frac{\mu_f}{\epsilon_f}} \ln \frac{r_1}{r_2} \cong \frac{1}{2\pi} \sqrt{\frac{\mu_f}{\epsilon_f}} \ln \frac{r_o}{r_i} \tag{6}$$

Here μ_f and ϵ_f are the complex permeability and dielectric constant in mks units. ω is the frequency in radians/sec.

(7) Finally μ_f and ϵ_f are determined from equations (5) and (6):

$$\mu_f = \frac{2\pi \gamma_f Z_{of}}{j\omega \ln \frac{r_o}{r_i}} = \mu_o (\mu_1 - j\mu_2) \tag{7}$$

$$\epsilon_f = \frac{\gamma_f \ln \frac{r_o}{r_i}}{2\pi j\omega Z_{of}} = \epsilon_o (\epsilon_1 - j\epsilon_2) \tag{8}$$

$$\mu_o = \frac{4\pi}{10^7} \; ; \qquad \epsilon_o = \frac{1}{36\pi 10^9}$$

μ_1, μ_2, ϵ_1, and ϵ_2 are the constants relative to free space.

The coaxial line we have is unfortunately not an ideal line. It suffers in the following respects:

(1) The shorting plunger cannot be positioned adjacent to the ferrite sample because the grounding fingers protrude beyond the leading

face of the plunger. It is hoped this can be corrected without resorting to the necessary corrections in the formulas above.

(2) There is a 1/2 inch taper in the inner and outer conductors that may introduce error. However, since 1/2 inch is so short compared to a wave length, the effect of the taper should be negligible.

(3) The axial slots necessary to make the walls of the line flexible have a small but negligible effect on the characteristic impedance of the line.

To date the line has not been placed in service. Some difficulties have been encountered and are in the process of solution. It should be pointed out that this method is long and involved. However, it is justified for the reasons enumerated in QPR No. 3.

<u>3.7.3 Coaxial Inductor No. 2.</u> A second coaxial inductor similar to that described in QPR No. 3 has been designed. The length of 50 ohm line joining the bridge's impedance-measuring elements and the inductor No. 1 cavity had necessitated a transmission line correction by means of the Z-ϕ chart. Since this is a time consuming operation, the length of line was reduced in the new design from 8 to 3.5 cm. One can correct for such a short line without resort to the Z-ϕ chart except at the high end of the frequency band. Unfortunately this inductor is not satisfactory. It behaves as if it were approaching a resonance. The apparent inductance of the empty inductor increased with frequency.

This behavior is similar to that of a tank circuit at frequencies below resonance. Fig. 8 is a drawing of the second coaxial inductor. The capacitances which may be responsible for the increase in apparent inductance are shown. Coaxial Inductor No. 1 showed no such effect, since a taper section was used, minimizing the effect of shunting capacitances.

3.7.4 The Z-Ø Chart. The Z-Ø chart, 24 inches in diameter, has been in use throughout the quarter. The formula used in calculating the chart was:[4]

$$\frac{Ze^{j\phi}}{Z_o} = \frac{1 + x + jy}{1 - x - jy} \tag{9}$$

where y and x are the ordinate and abscissa measured from the center of the chart. Z_o is the characteristic impedance (50 ohms). Contours of constant Z and of constant Ø were plotted.

3.8 Hall Effect (B. Hershenov)

A specimen has been placed in the magnet for measurement of the Hall emf. A determination has not been made as there were a few troubles located in the equipment. The majority of these failures have been located and remedied. One major difficulty remains and is located in the bucking section of QPR No. 1, P 36-37. The 60 cps pickup in the Hall circuit is balanced out without any difficulty. The 60 cps. pickup in the driver output is negligible so that the pickup loop made from one of the leads connecting the power amplifier to the primary electrodes is not necessary. This was not true for an n-type germanium specimen which was first inserted for a test run. However, the leads from

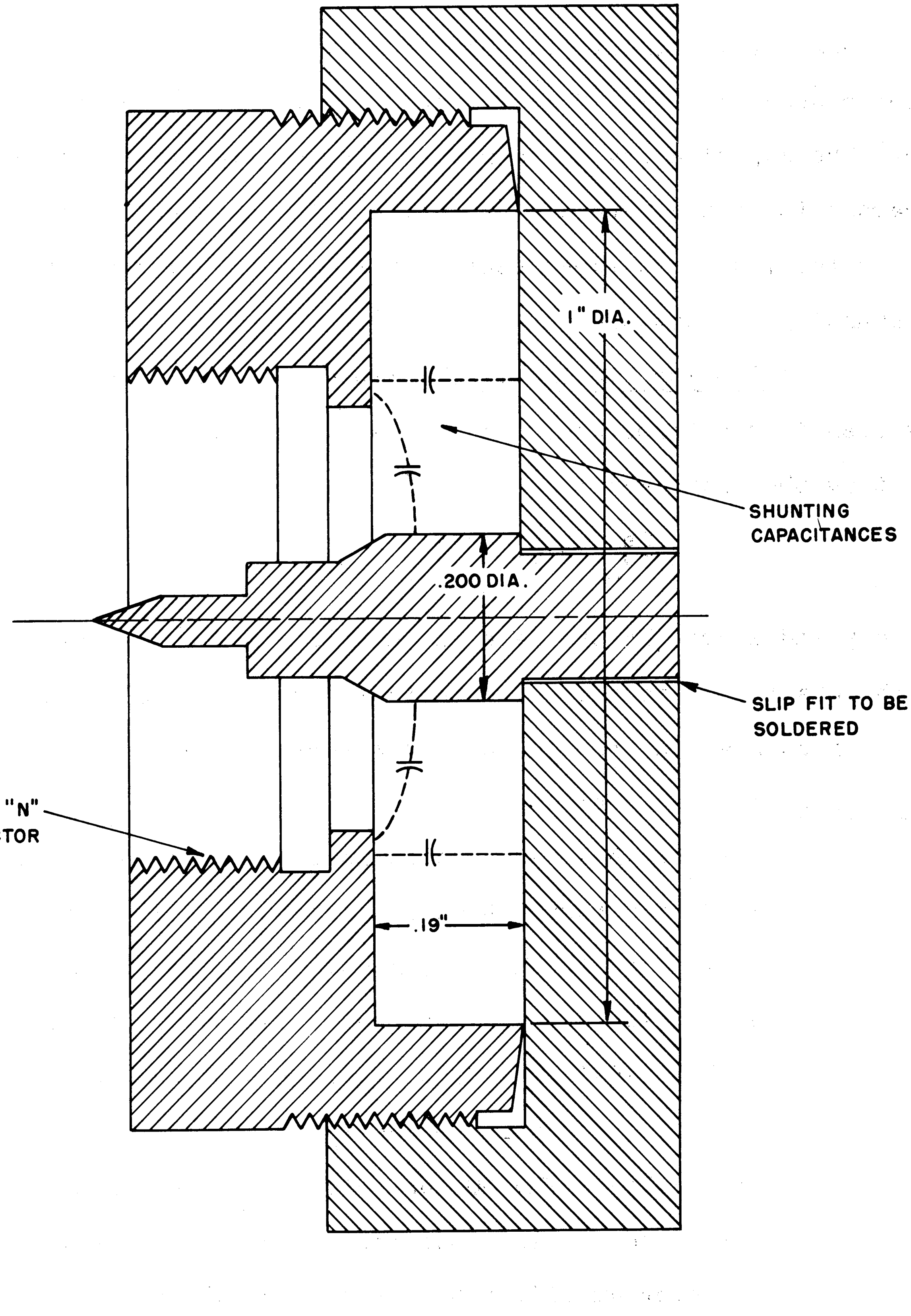

FIG. 8

COAXIAL INDUCTOR #2 ASSEMBLY.

the primary electrodes on the ferrite specimen are fixed to form a figure eight with the specimen body and this has eliminated any detectable 60 cps in the driver output. It has not been possible to balance out the 85 cps signal in the Hall circuit with the bucking section. The 85 cps signal of the bucking section is provided by a transformer in parallel with the output transformer. A measurement of this input indicates that it is about 10% of the primary voltage, as it should be. The amplifier adjustment is made with a 50Ω precision potentiometer with a minimum resistance increment of 5×10^{-5} times its total resistance. This resistor is reading properly. It will be necessary to check the sine-cosine resolver unit for the apparent lack of 85 cps for bucking. Once this has been remedied readings can be taken.

3.9 Magnetostriction (D. W. Martin)

No work was done on magnetostriction during the quarter. Work was concentrated on Sec. 3.3. This program will be resumed when that of Sec. 3.3 is completed.

3.10 Specific Heat of the Ferrite Materials (D. M. Grimes)

Since the measurement of the specific heat involves considerable effort, the measurement on one of our own samples has been suspended until the results of the analysis of Sec. 3.5 are known.

Work is continuing on the manufacture of very pure Fe_2O_3.

No further work on the specific heat in the region of sublattice alterations has been done.

4. CONCLUSIONS

The discrepancy between J_s as measured around the toroid and across it has been partially accounted for. With the new magnet we are able to obtain quite accurate readings around the loop.

From the differential equations of Sec. 3.2 we expect additional tuning range, which is intuitively obvious, and also a "tuning catastrophe".

We have found that the closer temperature control afforded by our new oven, and a slow rate of heating through:

(a) 100° C (voltalize water)

(b) 270° C (voltalize binder)

(c) 950° C - 1200° C (core shrinkage)

has allowed us to produce uniformally good physical properties.

5. PROGRAM FOR THE NEXT INTERNAL

All work reported on is to be continued. More time is to be devoted to the Hall Effect by Mr. Hershenov. Mr. Nace in addition to his high frequency measurements will test the equations of Section 3.2. Mr. Martin, now that the J_s discrepancy is nearly understood, will turn over routine measurements to a technician and set up the magnetostriction measuring strain gauges. Mr. Jefferson will embark on a program of internal stress analysis. Low frequency dielectric constant measurement is being by passed temporarily.

It is expected that the new specific heat measurement will be made shortly by Dr. Westrum.

REFERENCES

1. Brown, William Fuller, Jr.
   Domain Theory of Ferromagnetics Under Stress
   I. Phys Rev 52, 325-334 (1937)
   II. Phys Rev 53, 482-491 (1938)
   III. Phys Rev 54, 279-287 (1938)
   Theory of Reversible Magnetization in Ferromagnetics
   Phys Rev 55, 568-578 (1939)

2. Reference Data for Radio Engineering, Federal Telephone and Radio Corporation (1949), American Book-Stratford Press. Pg. 313

3. Ramo and Whinnery, Fields and Waves in Modern Radio, Wiley and Sons, (1944), Pg. 332-333

4. Bronwell and Beam, Theory and Application of Microwaves, McGraw Hill, (1947) Pg. 167

DISTRIBUTION LIST

1 Copy	Director, Electronic Research Laboratory Stanford University Stanford, California Attn: Dean Fred Terman
1 Copy	Commanding Officer Signal Corps Electronic Warfare Center Fort Monmouth, New Jersey
1 Copy	Chief, Engineering and Technical Division Department of the Army Washington 25, D. C. Attn: SIGGE-C
1 Copy	Chief, Plans and Operations Division Office of the Chief Signal Officer Washington 25, D. C. Attn: SIGOP-5
1 Copy	Countermeasures Laboratory Gilfillan Brothers, Inc. 1815 Venice Blvd. Los Angeles 6, California
1 Copy	Commanding Officer White Sands Signal Corps Agency White Sands Proving Ground Las Cruces, New Mexico Attn: SIGWS-CM
1 Copy	Signal Corps Resident Engineer Electronic Defense Laboratory P. O. Box 205 Mountain View, California Attn: F. W. Morris, Jr.
1 Copy	Mr. Peter H. Haas High Frequency Standard Section Central Radio Propagation Laboratory National Bureau of Standards Washington 25, D. C.
75 Copies	Transportation Officer, SCEL Evans Signal Laboratory Building No. 42, Belmar, New Jersey For - Signal Property Officer Inspect at Destination File No. 25052-PH-51-91(1443)

1 Copy	W. G. Dow, Professor Dept. of Electrical Engineering University of Michigan Ann Arbor, Michigan
1 Copy	H. W. Welch, Jr. Engineering Research Institute University of Michigan Ann Arbor, Michigan
1 Copy	Document Room Willow Run Research Center University of Michigan Willow Run, Michigan
10 Copies	Electronic Defense Group Project File University of Michigan Ann Arbor, Michigan
1 Copy	Engineering Research Institute Project File University of Michigan Ann Arbor, Michigan